Translational autoregulation of RF2 protein in *E. coli* through programmed frameshifting

Ajeet K. Sharma*
Department of Physics, Indian Institute of Technology, Jammu 181221, India

(Received 6 April 2020; revised 20 February 2021; accepted 4 June 2021; published 21 June 2021)

Various feedback mechanisms regulate the expression of different genes to ensure the required protein levels inside a cell. In this paper, we develop a kinetic model for one such mechanism that autoregulates RF2 protein synthesis in *E. coli* through programmed frameshifting. The model finds that the programmed frameshifting autoregulates RF2 protein synthesis by two independent mechanisms. First, it increases the rate of RF2 synthesis from each mRNA transcript at low RF2 concentration. Second, programmed frameshifting can dramatically increase the lifetime of RF2 transcripts when RF2 protein levels are lower than a threshold. This sharp increase in mRNA lifetime is caused by a first-order phase transition from a low to a high ribosome density on an RF2 transcript. The high ribosome density prevents the transcript's degradation by shielding it from nucleases, which increases its average lifetime and hence RF2 protein levels. Our study identifies this quality control mechanism that regulates the cellular protein levels by breaking the hierarchy of processes involved in gene expression.

DOI: 10.1103/PhysRevE.103.062412

I. INTRODUCTION

Proteins perform numerous cellular functions including genome regulation, cellular metabolism, and transport and storage of nutrients [1–3]. Cells require a precise concentration of different protein molecules, and any dysregulation in the production of these proteins can lead to many abnormalities and several types of diseases [4–6]. Cells regulate protein levels under different conditions through various feedback mechanisms acting at both transcriptional and translational levels [7–9]. Release factor 2 (RF2) protein in *E. coli* is one of the essential proteins whose expression is tightly regulated through a negative feedback mechanism [10]. This protein terminates the process of protein synthesis in *E. coli* transcripts with UAA and UGA stop codons [11]. Therefore, any dysregulation in the synthesis of RF2 protein may severely affect the expression of several other genes in *E. coli*.

The RF2 protein level in *E. coli* is regulated by a mechanism called programmed frameshifting [10,12]. Frameshifting is a process in which a ribosome slides by one or more nucleotides in either the forward or backward direction without adding or removing any amino acid into the nascent protein it is synthesizing. This unusual sliding of ribosomes changes the transcript's codon composition for the frameshifted ribosomes. The *E. coli* RF2 transcript is a 366-codon-long transcript which has UGA stop codons at the 26th and 366th codon positions. When RF2 proteins are present in an abundant amount, they are readily available for a ribosome to quickly terminate the translation process at the 26th codon position, producing a small protein (SP) of 25 amino acids. The 26th codon of the RF2 transcript is preceded by the CUU codon. Its combination with the adjoined UGA codon can frameshift a ribosome by +1 nucleotide [10]. Therefore, a lower concentration of RF2 protein, which makes the ribosome wait longer at the 26th codon position, leads to a more frequent frameshifting [Fig. 1(a)]. This programmed frameshifting allows the ribosomes to bypass the first stop codon; therefore, it terminates the translation at the next stop codon of the transcript. Note that this frameshifted sequence code is for the 365-amino-acid-long RF2 protein. This means the frameshifting caused by a lower concentration of RF2 protein enhances its production.

The ribosome density on an *E. coli* transcript can significantly affect its lifetime. A high ribosome density shields mRNA molecules from nucleases and thus increases their average lifetime [13–16]. The RF2 protein concentration can regulate the ribosome density on an RF2 transcript through the frameshifting mechanism as it controls the entry of ribosomes after the 26th codon position of the transcript [10]. This means that RF2 protein levels in *E. coli* can also affect the average lifetime of the RF2 transcript and thus the overall production rate of RF2 proteins. Although the role of programmed frameshifting in regulating RF2 protein synthesis by controlling the entry of ribosomes at the first stop codon is well understood [10], its impact on the overall rate of RF2 synthesis through mRNA lifetime remains unknown.

In this study, we develop a kinetic model for translational autoregulation of RF2 protein synthesis in *E. coli*. The model captures the effect of programmed frameshifting on mRNA lifetime and the overall synthesis rate of RF2 proteins. We find that lowering the RF2 concentration in *E. coli* leads to a sharp increase in the average lifetime of the RF2 transcripts. Similarly, a high RF2 concentration decreases mRNA lifetime by a significant amount. This means that, when required, frameshifting can dramatically increase or decrease the production of RF2 proteins by regulating the average lifetime of RF2 transcripts.

II. MODEL

A. Model of protein synthesis and mRNA degradation

We used a previously developed inhomogeneous ℓ–totally asymmetric simple exclusion process (ℓ-TASEP) model to

*ajeet.sharma@iitjammu.ac.in

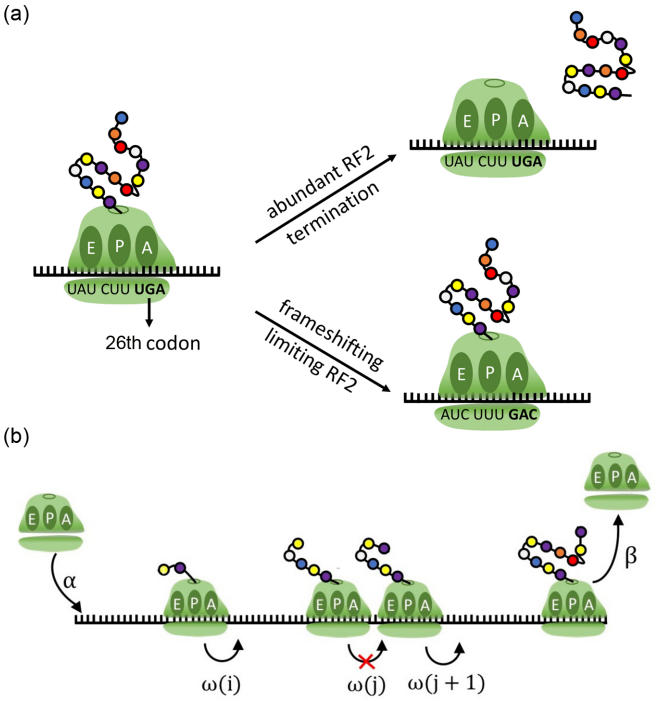

FIG. 1. Schematic of programmed frameshifting and the process of protein synthesis. (a) A limiting concentration of RF2 proteins allows the ribosomes to spend more time on the UGA codon at the 26th position of the RF2 transcript, thus increasing the chances of frameshifting as the combination of CUUUGA nucleotides (25–26 codons) promotes +1 frameshifting. The frameshifting changes the A-site codon from UGA to GAC (shown in bold font). An abundance of RF2 proteins quickly terminates the protein synthesis at the 26th codon position and releases a 25-amino-acid-long short protein. (b) A ribosome initiates the process of protein synthesis with rate α when the first six codon positions of the transcript are not occupied by other ribosomes. Then the ribosome moves stochastically by taking irreversible steps towards the stop codon. The step from codon j to $j+1$ occurs with rate $\omega(j)$. Note that a ribosome cannot move forward if its passage is occupied by another ribosome on the same transcript. A ribosome terminates protein synthesis with rate β after it reaches the stop codon.

simulate protein synthesis on the *E. coli* RF2 transcript [17–23]. In this model, a ribosome covers ℓ consecutive codon positions of a transcript. A ribosome initiates protein synthesis in this model when the first five codon positions after the start codon are not occupied by other ribosomes [24,25]. This step occurs with rate α, which correlates positively with the availability of free ribosomes in a cell [26]. In our model, we assume that ribosome concentration is in a steady state; therefore, the initiation rate does not change with time. After initiation, a ribosome starts sliding along the mRNA sequence by taking stochastic steps from the start to the stop codon. The ribosome moves from the codon position j to $j+1$ with rate $\omega(j)$. (Note that we use the position of the ribosome A-site to indicate its location on the transcript.) In each such step, ribosomes elongate the nascent protein by one amino acid subunit [Fig. 1(b)]. A ribosome cannot move to the next codon if that codon is occupied by another downstream ribosome. When a ribosome arrives at the stop codon it terminates the process and releases the fully synthesized protein with rate β.

We incorporated programmed frameshifting in our model by allowing the possibility of two competing transitions when the ribosome is at the 26th codon position of the RF2 transcript. At the 26th codon position, a ribosome can either terminate the protein synthesis process with rate β or frameshift by one nucleotide with rate k_{frame}.

During translation, ribosomes moving on an mRNA transcript shield that molecule from nucleases, restricting their access for mRNA degradation [13–16]. To incorporate this phenomenon in our simulation model, we used an approach that is inspired by a previously published study [13]. We assumed that two different types of mechanisms degrade an mRNA molecule. First, nucleases bind to the portions of an mRNA transcript that are not covered by any ribosome and then degrade the molecule [13–16]. The degradation rate from this mechanism for a transcript with N_s nucleotides exposed to nucleases is $k_{d1}(0)N_s$, where $k_{d1}(0)$ is the degradation rate per nucleotide (not covered by the ribosomes). Second, mRNA degradation independent of the ribosome density occurs at a constant rate of k_{d2} [27].

B. Simulation procedure

Protein synthesis simulations from the ℓ-TASEP model require the initiation rate, the termination rate, and the translation rate of each codon of the RF2 transcript. In our simulations, we set the initiation rate α equal to 0.33 s^{-1} [13]. Translation termination in *E. coli* is a multistep process and follows Michaelis-Menten kinetics [28,29]. Therefore, the termination rate β has the following dependence on RF2 concentration:

$$\beta = \frac{V_{\max}[\text{RF2}]}{[\text{RF2}] + K_M}, \tag{1}$$

where K_M is the Michaelis constant and $V_{\max}$ is the termination rate when the RF2 concentration is much larger than K_M [30]. We use the translation rates of all 61 sense codons which were reported in a previously published study [31]. The minimum and maximum codon translation rates on the RF2 transcript were 2.45 and 54.04 s^{-1}, respectively, whereas the ratio of the standard deviation to the mean codon translation rate was 0.69. In our simulations, we set $k_{d1}(0) = 0.000\,05$ s^{-1} and $k_{d2} = 0.0005$ s^{-1}. The numerical values of $k_{d1}(0)$ and k_{d2} are chosen such that our simulations give the lifetime of the RF2 transcript in a physiologically permissible range for *E. coli* mRNA molecules [13]. We simulate protein synthesis and mRNA degradation on the RF2 transcript by using the Gillespie's method [32], whose details are provided in the Supplemental Material [33]. The numerical values of all simulation parameters are given in Table I.

To measure the rate of SP and RF2 synthesis in our simulations, we set all degradation rates to zero. We then start the measurement of the time taken to synthesize 10 000 copies of RF2 proteins and SP after the translation system achieves a steady state. We divide the total number of copies of SP and RF2 proteins by the time taken to synthesize them to get the numerical values of J_1 and J_2, respectively.

TABLE I. Parameters used in the simulation.

Parameter	Description	Value	Reference
K_M	Michaelis constant for translation termination	0.5–10 μM	[29]
$V_{\max}$	termination rate when RF2 concentration is very large	5 s^{-1}	[29]
ℓ	number of codons covered by a ribosome	10	[34]
k_{frame}	frameshifting rate	1–40 s^{-1}	varied to access the robustness of results
$k_{d1}(0)$	ribosome-density-dependent degradation rate (per nucleotide)	0.00003–0.0003 s^{-1}	estimated (see the text for details)
k_{d2}	ribosome-density-independent degradation rate	0.0002–0.002 s^{-1}	estimated (see the text for details)
k_d^{SP}	degradation rate of SP	10^{-4} s^{-1}	[35,36]
k_d^{RF2}	degradation rate of RF2 protein	10^{-4} s^{-1}	[35,36]
k	production rate of RF2 mRNA	10^{-2} s^{-1}	[45]
α	translation initiation rate	0.33 s^{-1}	[13] (see the text for details)
$\omega(j)$	codon translation rate	2.45–54.04 s^{-1}	[31]

To measure the average mRNA lifetime at a specific RF2 concentration, we simulate protein synthesis on an RF2 transcript until that transcript is degraded. We repeat this procedure 10 000 times and calculate the average mRNA lifetime at a given steady-state RF2 concentration. We calculate the average mRNA lifetime for RF2 concentrations varying from 10 nM to 1000 nM. The effect of changing the steady-state RF2 concentration in our simulations is captured by varying the termination rate according to Eq. (1).

III. RESULTS

A. A high RF2 concentration in *E. coli* decreases its production

It has been shown that RF2 proteins can autoregulate their concentration in *E. coli* through a negative feedback mechanism [12]. We first examine whether our model can reproduce this experimentally observed behavior of RF2 protein synthesis. To do that, we define a parameter

$$\gamma = \frac{J_2}{J_1 + J_2}, \tag{2}$$

where J_1 and J_2 are the rates of SP and RF2 synthesis from a single copy of the transcript, respectively. The parameter γ is the relative rate at which RF2 proteins are produced under steady-state conditions. We compute the numerical values of J_1 and J_2 using the procedure described in Sec. II and calculate γ using Eq. (2). We plot γ as a function of the steady-state RF2 concentration for the frameshifting rates varying from 1 s^{-1} to 40 s^{-1} (Fig. 2). We find that for all frameshifting rates, the relative rate of RF2 production decreases monotonically as a function of its steady-state concentration. This monotonic decrease in γ can be explained by a decrease in the frameshifting probability of ribosomes as RF2 concentration increases. At high RF2 concentration, it is readily available to terminate the translation process when the ribosome encounters the first stop codon at the 26th codon position of the transcript, thus reducing the chances of frameshifting and decreasing the rate of RF2 production [Fig. 1(a)]. We also find that a lower frameshifting rate leads to a sharper transition from a high rate to a low rate of RF2 production (Fig. 2). This observation can be explained by a very simple model of competition between the termination of SP and programmed frameshifting [Fig. 1(a)]. In this simple model, J_1 and J_2 are proportional to β and k_{frame}, respectively. Therefore,

$$\gamma = \frac{J_2}{J_1 + J_2} = \frac{k_{\text{frame}}}{\frac{V_{\max}[\text{RF2}]}{K_M + [\text{RF2}]} + k_{\text{frame}}}. \tag{3}$$

We plot γ calculated from Eq. (3) as a function of steady-state RF2 concentration and find an excellent agreement with our simulation results (solid lines in Fig. 2). Equation (3) also explains that if we have a lower k_{frame} value, then the relative contribution of J_2 in J decreases more sharply as a function of [RF2], resulting in a sharper decrease in γ. These results are qualitatively similar to those reported in Ref. [12], suggesting that our detailed kinetic model can quantitatively describe the dependence of the steady- state RF2 protein concentration on the rate of RF2 synthesis from a single transcript.

B. A high RF2 protein concentration decreases the average lifetime of RF2 transcripts

It has been shown experimentally that the ribosome coverage on *E. coli* transcripts can significantly impact their

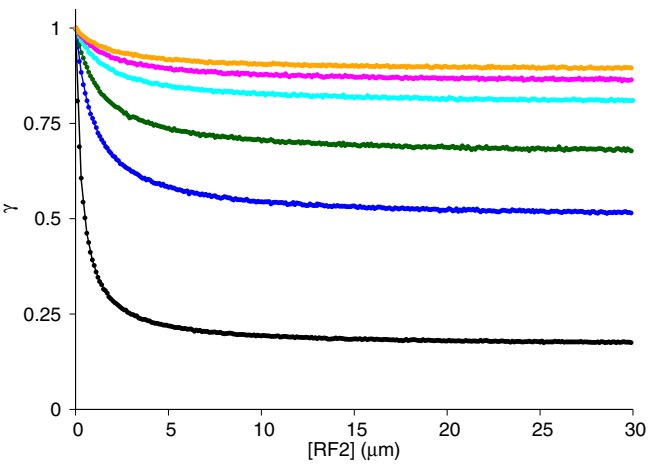

FIG. 2. A higher RF2 concentration decreases its production. The relative production of RF2 protein is plotted against the steady-state RF2 concentration for $k_{\text{frame}} = 1,\ 5,\ 10,\ 20,\ 30$, and 40 s^{-1} in black, blue, green, cyan, magenta, and orange, respectively. The discrete data points are obtained from the simulations of RF2 protein synthesis whereas the solid lines are plotted using Eq. (3).

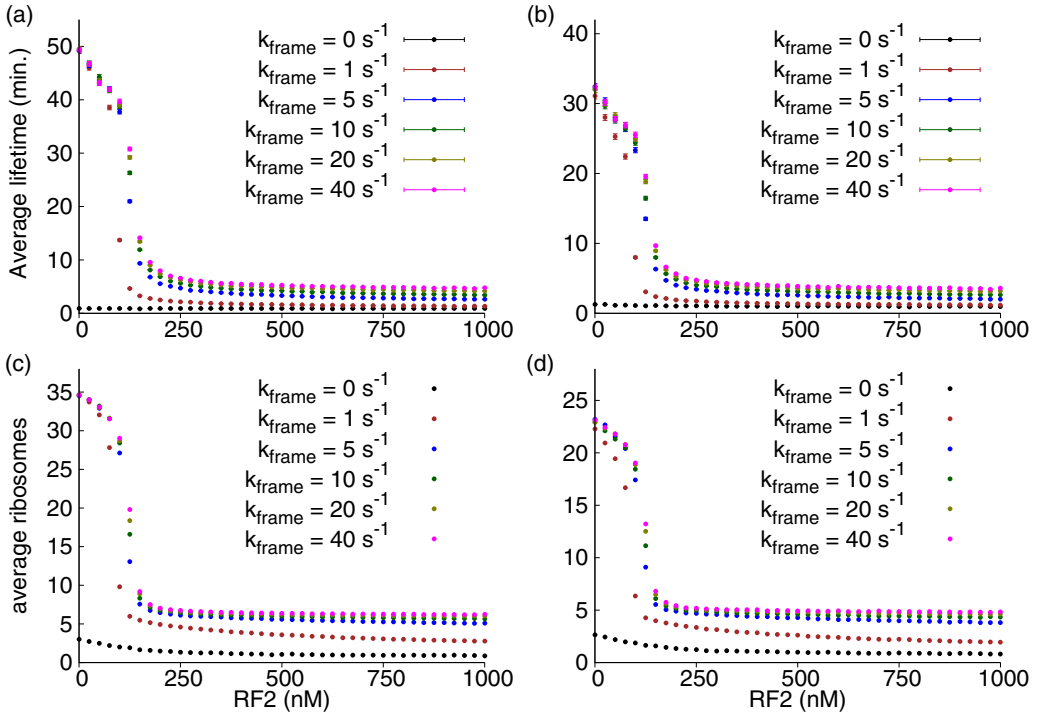

FIG. 3. An increase in RF2 concentration decreases the lifetime of the RF2 transcript. (a) and (b) Average mRNA lifetime of the RF2 transcript plotted against the steady-state RF2 concentration in *E. coli*. The error bars in (a) and (b) represent the standard error in the measurement of mRNA lifetime with 95% confidence interval. (Note that the error bars in (a) and (b) are smaller than the size of the data point.) (c) and (d) Average number of ribosomes on the RF2 transcript plotted against the RF2 concentrating in *E. coli.* In (a) and (c) we start mRNA degradation in our simulation after the translation system achieves steady-state conditions, whereas in (b) and (d) we start it from $t = 0$.

lifetime [13–16]. The ribosome coverage over mRNA shields the molecules from nucleases and thus prevents their degradation. Frameshifting rate and RF2 concentration are the two quantities that determine the average number of ribosomes on an RF2 transcript after the 26th codon position (Fig. 1). This suggests that these two parameters can also influence an RF2 transcript's lifetime and thus can affect RF2 protein levels in *E. coli*. To understand the effects of RF2 protein concentration on the RF2 transcript's lifetime, we simulate protein synthesis on an RF2 transcript and its degradation using the procedure described in Sec. II. In our simulations, we first wait for the translation system to achieve a steady state and then introduce degradation in our simulations. We calculate the average lifetime of the RF2 transcript for steady-state RF2 concentrations varying from 10 nM to 1000 nM. We find that initially increasing the steady-state RF2 concentration gradually decreases the average lifetime of the RF2 transcript [Fig. 3(a)]. Then we see a sharp decrease in mRNA lifetime at a specific RF2 concentration, which again saturates as we further increase the steady-state RF2 concentration. This sharp decrease in the RF2 transcript's average lifetime can be explained by a sharp decrease in the average ribosome density, which exposes the mRNA molecules to nucleases and thus dramatically decreases the transcript's lifetime [Fig. 3(c)].

The sharp decrease in the average ribosome density in Fig. 3(c) is a result of the discontinuous transition from a high density (HD) to a low density (LD) of ribosomes in the inhomogeneous ℓ-TASEP model [21,37]. Note that the termination of protein synthesis at the 26th and 366th codon positions for SP and RF2 proteins, respectively, occurs through the UGA codon. The termination rate at the UGA codon has a Michaelis-Menten-like dependence on RF2 concentration [Eq. (1)] [11]. Therefore, a slower termination rate caused by the lower RF2 concentration frameshifts ribosomes at the 26th codon position [Fig. 1(a)], but also creates a blockage of ribosomes at the second stop codon. This blockage at the second stop codon creates a HD-like regime on the RF2 transcripts. Note that any increase in the RF2 concentration increases the termination rate β [Eq. (1)], thus decreasing the ribosome density by relieving the ribosome traffic jams at the second stop codon, which switches the translation system to the LD regime [18,21].

In Fig. 3(a) we start mRNA degradation in our simulations only after the translation system achieves a steady state. However, mRNA degradation can start before the translation system reaches a steady state. Therefore, we also investigate the effects of RF2 concentration on an RF2 transcript's lifetime under non-steady-state conditions where mRNA degradation starts at $t = 0$. We find that the switching from a long to a short mRNA lifetime under non-steady-state conditions remains qualitatively similar to the steady-state ones [Figs. 3(b) and 3(d)]. However, the average mRNA lifetime in the non-steady-state conditions is slightly lower than that in the steady state, because in the former case, a larger portion of the mRNA transcript remains exposed to nucleases before the translation system evolves to a steady state.

We also find that the behavior of the mRNA lifetime as a function of RF2 concentration does not change much while

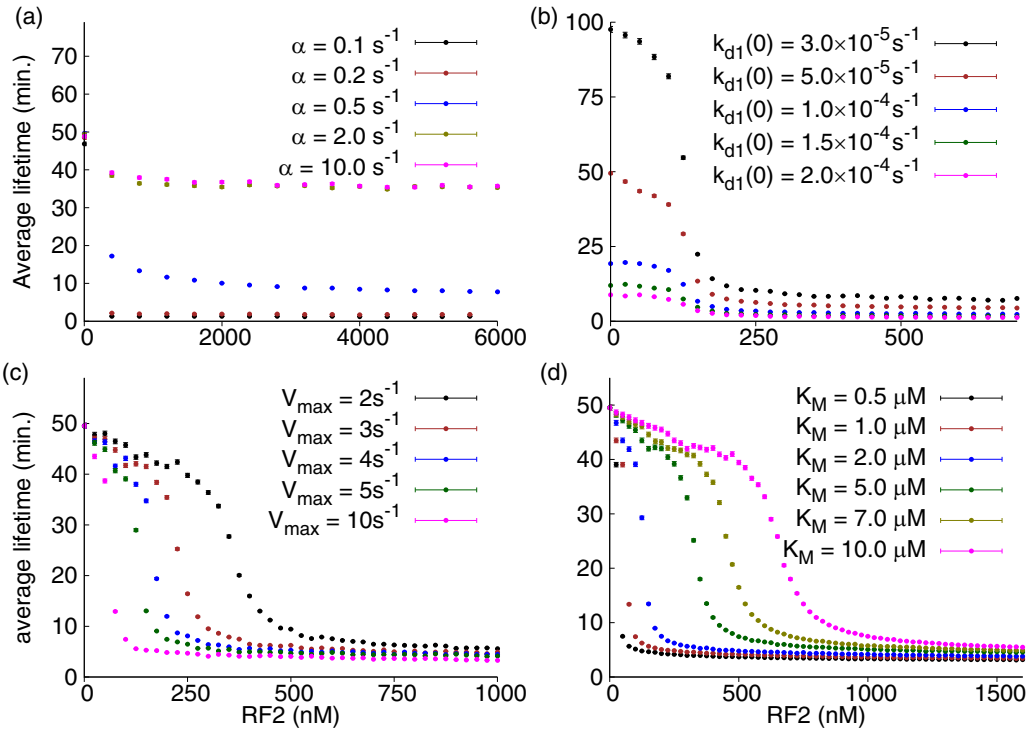

FIG. 4. The transition from a long to a short mRNA lifetime remains robust against any changes in the mRNA degradation and translation termination rates. The average lifetime of the RF2 transcript against steady-state RF2 protein concentration is plotted for (a) varying initiation rate α, (b) $k_{d1}(0)$ and k_{d2}, (c) maximum termination rate $V_{\max}$, and (d) Michaelis constant K_M. The error bars represent the standard error in the measurement of mRNA lifetime with 95% confidence interval. Note that the error bars in this figure are smaller than the size of the data point.

varying the frameshifting rate (Fig. 3). This is because the ribosome density that regulates the RF2 transcript's lifetime in the HD and LD regimes is mainly determined by the initiation and termination rates, respectively [18,21]. Thus, the effect of any changes in the frameshifting rate on the average ribosome density and RF2 transcript's lifetime remains minimal (Fig. 3).

C. Switching from the long to the short mRNA lifetime is robust against any changes in most of the rate parameters

We find that decreasing the RF2 concentration from a threshold causes a sharp increase in the mRNA lifetime (Fig. 3). This behavior of the mRNA lifetime can be a consequence of a specific set of parameter values that we used in our simulations. Therefore, we also assess how the mRNA lifetime behavior changes under different conditions by changing various rate parameters in our simulations.

The switching from the LD regime to the HD regime is responsible for a sharp transition from a short to a long mRNA lifetime as RF2 concentration decreases (Fig. 3). This sharp transition between the LD and HD regimes occurs when the RF2 transcript has an initiation rate that is lower than the termination and average elongation rates [21,37]. Because, at a high initiation rate, protein synthesis on a transcript occurs either in the HD or in the maximal current (MC) regime [18]. (Note that the ribosome density in the MC regime is between the LD and HD regimes [37].) If the translation system is in the MC regime, then any decrease in the termination rate may lead to a transition from the MC to the HD regime, which is a continuous phase transition [18]. Therefore, we do not find a sharp transition from a short to a long mRNA lifetime at a high initiation rate [Fig. 4(a)]. This result shows that a low translation-initiation rate is an essential requirement for a sharp switchlike transition in the average lifetime of the RF2 transcript.

We also test the robustness of switching from the short to the long mRNA lifetime against varying degradation rates, i.e., $k_{d1}(0)$ and k_{d2}. We vary $k_{d1}(0)$ and k_{d2} in our simulations from 0.000 03 and 0.0003 s^{-1} to 0.0002 and 0.002 s^{-1}, respectively, and find an increase in the average mRNA lifetime without changing the transition point between the two phases of the mRNA lifetime [Fig. 4(b)]. This behavior of the mRNA lifetime is expected because degradation rates cannot change the ribosome coverage on an RF2 transcript. It can only increase or decrease the nuclease activity, which leads to a slower or faster degradation of mRNA molecules, respectively. The other two parameters that can significantly affect the degradation rate are $V_{\max}$ and K_m [Eq. (1)]. Increasing $V_{\max}$ or decreasing K_M increases the termination rate β [Eq. (1)] at a given RF2 concentration. Therefore, the translation system requires lower RF2 concentration to switch from the HD- to the LD-like regime [Figs. 4(c) and 4(d)].

Ribosome hydrolyzes the GTP molecule in each step it takes to incorporate an amino acid into the growing nascent protein [38–40]. Energy expenditure has been shown to enhance the efficiency of decision-making in various biological processes [41–43]. The autoregulation of the RF2

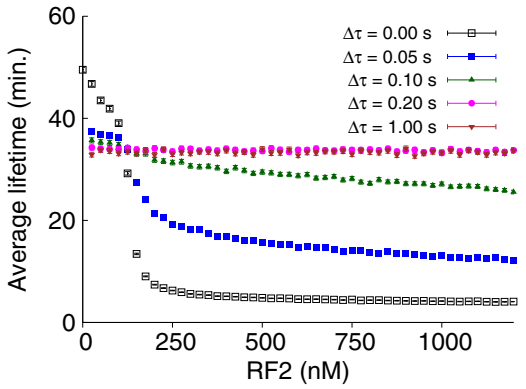

FIG. 5. Energy expenditure increases the efficiency of switching between a short and a long RF2 lifetime. The average lifetime of the RF2 transcript is plotted against the steady-state RF2 concentration for varying GTP concentration in *E. coli*. The effect of varying the GTP concentration is captured by increasing the translation time of each codon in a transcript by 0.05, 0.10, 0.20 and 1.00 s. The error bars in this figure represent the standard error in the measurement of mRNA lifetime with 95% confidence interval. (Note that the error bars are smaller than the size of the data points.)

synthesis is also a decision-making process that allows switching between a long and a short mRNA lifetime. Therefore, we test the role of energy expenditure in RF2 autoregulation by varying the GTP concentration in our simulations. Note that the GTP molecule is supplied to a ribosome through the elongation factors EF-G and EF-Tu [38,39]. Therefore, decreasing the GTP concentration decreases the availability of these two complexes in the ribosome elongation cycle. To mimic a decrease in the GTP concentration in our simulations, we construct four new translation rate profiles by increasing the translation time of each codon by 0.05, 0.10, 0.20, and 1.00 s. Then we test how this uniform increase in codon translation time affects the switching between the short and the long mRNA lifetime as a function of steady-state RF2 concentration. We find that switching between the short and the long mRNA lifetime gradually disappears when the GTP concentration decreases (Fig. 5). This happens because at low average codon translation rates, protein synthesis occurs in the MC regime [37]. Therefore, decreasing the RF2 concentration leads to a continuous transition from the MC- to the HD-like regime (Fig. 5).

This analysis shows that the transition from a short to a long mRNA lifetime, caused by the programmed frameshifting, is not affected by any changes in the degradation rate and translation termination kinetics. However, increasing the initiation rate or decreasing the codon translation rate may disrupt the sharp transition between the long and the short lifetime of the RF2 transcript. These results also show that energy expenditure increases the efficiency of switching between the short and the long lifetime of the RF2 transcript.

D. Programmed frameshifting ensures stable RF2 protein levels in *E. coli*

The average lifetime of the RF2 transcript dramatically increases when the RF2 concentration decreases from a threshold value (Fig. 3). This increase in the average lifetime of the RF2 transcript must contribute positively to the overall rate of RF2 protein synthesis [44]. However, a lower RF2 concentration leads to a slower termination rate [Eq. (1)], thus decreasing the rate of RF2 synthesis from a single transcript. Therefore, we test how these two competing factors determine the overall rate of RF2 synthesis as a function of steady-state RF2 concentration. To do that, we derive three chemical kinetic equations that govern the concentrations of SP, RF2, and RF2 transcripts in *E. coli*:

$$\frac{d[\mathrm{SP}]}{dt} = [m]J_1 - [\mathrm{SP}]k_d^{\mathrm{SP}} = \frac{[m]J}{1+\frac{k_{\mathrm{frame}}}{\beta}} - [\mathrm{SP}]k_d^{\mathrm{SP}}, \tag{4}$$

$$\frac{d[\mathrm{RF2}]}{dt} = [m]J_2 - [\mathrm{RF2}]k_d^{\mathrm{RF2}} = \frac{[m]\,J}{1+\frac{\beta}{k_{\mathrm{frame}}}} - [\mathrm{RF2}]k_d^{\mathrm{RF2}}, \tag{5}$$

$$\frac{d[m]}{dt} = k - [m]k_d^m. \tag{6}$$

In Eqs. (4)–(6), [SP], [RF2], and $[m]$ denote the concentrations of SP, RF2, and RF2 transcripts, respectively. The termination rate β at a given RF2 concentration in Eqs. (4) and (5) is calculated using Eq. (1). In Eqs. (4) and (5), $[m]J_1$ and $[m]J_2$ are the gain terms that represent the net increase in [SP] and [RF2], respectively. The values of J_1 and J_2 in those equations are obtained from Eq. (3). In Eqs. (4) and (5), k_d^{SP} and k_d^{RF2} are the degradation rates for the SPs and RF2 proteins, respectively. The second term of these two equations accounts for a loss in the [SP] and [RF2] due to the protein degradation. In Eq. (6), k and k_d^m are the rates of RF2 mRNA synthesis and degradation, respectively. We set the RF2 transcript production rate k equal to 0.02 s^{-1} as this numerical value gives the steady-state mRNA copy numbers in a range that is typically found in *E. coli* [45]. Here k_d^m is the inverse of the average lifetime of the RF2 transcript and is obtained using the simulation procedure described in Sec. II (Figs. 3 and 4). The numerical values of the rate parameters used in Eqs. (4)–(6) are given in Table I.

We need the functional forms of J and k_d^m to numerically solve Eqs. (4)–(6). We obtain these functional forms by fitting the simulated values of J and k_d^m by the following piecewise functions of [RF2]:

$$J = \begin{cases} a[\mathrm{RF2}] & \text{if } [\mathrm{RF2}] \leqslant 0.14\ \mu\mathrm{M} \\ 0.26\ \mathrm{s}^{-1} & \text{if } [\mathrm{RF2}] > 0.14\ \mu\mathrm{M}, \end{cases} \tag{7}$$

$$k_d^m = \begin{cases} a_1 + b_1[\mathrm{RF2}] & \text{if } [\mathrm{RF2}] \leqslant 0.10\ \mu\mathrm{M} \\ \frac{a_2[\mathrm{RF2}]}{b_2+[\mathrm{RF2}]} & \text{if } [\mathrm{RF2}] > 0.10\ \mu\mathrm{M}. \end{cases} \tag{8}$$

We find that these functions fit well with simulated J and k_d^m (Figs. S1 and S2 in [33]). The two domains of J and k_d^m [Eqs. (7) and (8)] represent the HD- and LD-like regimes of ribosome traffic on the RF2 transcript (Figs. 3 and 4). At a low RF2 concentration, the translation system remains in the HD-like regime due to a low termination rate [Eq. (1)]. Therefore, increasing the RF2 concentration results in an increase in J [19,21]. However, a further increase in RF2 concentration transitions the translation system into the LD-like regime, where J is independent of the termination rate (Fig. S1 in [33]). Moreover, similar to the average mRNA lifetime

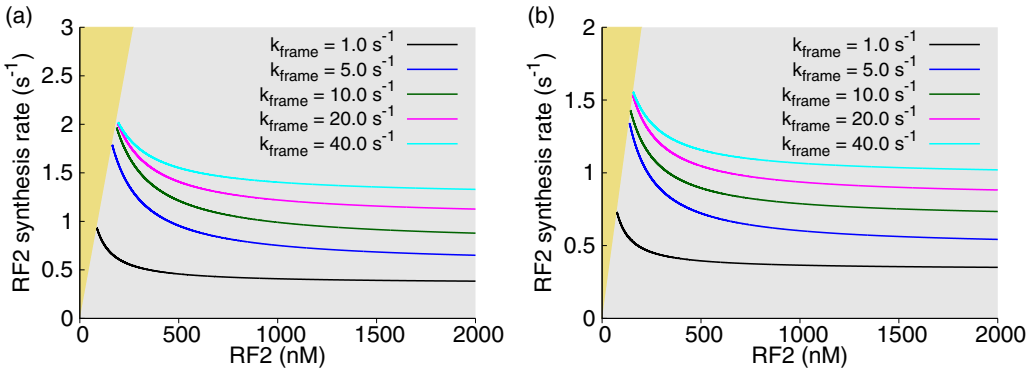

FIG. 6. An increase in RF2 concentration leads to a decrease in the overall production rate of RF2 proteins. The overall RF2 production rate (in number per second) is plotted against the steady-state concentration of RF2 proteins in *E. coli* for k_{frame} varying from 1 s^{-1} to 40 s^{-1} for (a) the steady-state case and (b) the non-steady-state case. The forbidden and allowed regions of the steady-state RF2 concentrations are shown in yellow and gray, respectively (see the text for details).

(i.e., the inverse of k_d^m), varying K_M and $V_{\max}$ also affects J (Figs. 4 and S3). Decreasing K_M or increasing $V_{\max}$ increases the termination rate; therefore, J becomes independent of the termination rate at a lower RF2 concentration (Fig. S3 in [33]).

We use the piecewise functions in Eqs. (7) and (8) as mathematical expressions for J and k_d^m, respectively, and numerically solve Eqs. (4)–(6) using the ode45 function of MATLAB 2019. Using numerical solutions, first we analyze how the steady-state concentrations of SP, RF2, and RF2 transcripts are affected by the initial conditions. To this end, we carry out an analysis by randomly choosing 10 000 different initial conditions and then use them to numerically solve Eqs. (5)–(8). We find that the steady-state concentrations of SPs, RF2 proteins, and RF2 transcripts are exactly the same for all 10 000 initial conditions. The steady-state concentrations of SPs and RF2 proteins are 7 and 40 μM, respectively, whereas it is 0.2 μM for RF2 transcripts. In Fig. S4 in [33] a few dynamic trajectories for RF2 proteins and SPs are plotted for different initial conditions of RF2 proteins.

Solving Eqs. (4)–(7), we calculate how the overall rate of RF2 synthesis varies as a function of steady-state RF2 concentration in *E. coli*. We change the steady-state concentration of RF2 proteins by varying the degradation rates k_d^{SP} and k_d^{RF2} from 0.0001 s^{-1} to 10.000 s^{-1}. We find that decreasing the steady-state RF2 concentration increases the overall rate of RF2 synthesis (Fig. 6). Interestingly, we also find that the steady-state RF2 concentration does not decrease beyond a threshold. We refer to the region beyond this threshold as the forbidden region. The only solution that is possible in the forbidden region has zero RF2 concentration. (Both forbidden and allowed regions of the steady-state RF2 concentrations are shown in yellow and gray in Fig. 6, respectively). Moreover, the lower bound on the allowed region of steady-state RF2 concentration increases with k_{frame} because increasing the frameshifting rate allows more ribosomes to synthesize RF2 protein.

We also test how translation rate parameters that affect the switching between a short and a long mRNA lifetime also affect the overall rate of RF2 synthesis. To do that, we calculate the overall rate of RF2 synthesis as a function of steady-state RF2 concentration for $V_{\max}$ and K_M varying from 2.0 s^{-1} to 10.0 s^{-1} and 0.5 μM to 10.0 μM, respectively. We find that the qualitative behavior of the rate of RF2 synthesis as a function of steady-state RF2 concentration remains robust against any changes in $V_{\max}$ and K_M (Fig. S5 in [33]). However, increasing K_M or decreasing $V_{\max}$ increases the lower bound for the allowed region of steady-state RF2 concentration. This increase in the lower bound for allowed RF2 concentration is caused by the increase in the RF2 concentration where the transition between the short and the long mRNA lifetime occurs [Figs. 4(c) and 4(d)].

Overall, these results show that the programmed frameshifting is a very efficient way to autoregulate the steady-state RF2 concentration in *E. coli*. The programmed frameshifting ensures stable RF2 levels by increasing the overall rate of RF2 synthesis when steady-state RF2 concentration decreases.

IV. DISCUSSION

RF2 is an essential protein in *E. coli* [46] and its concentration is tightly regulated through a negative feedback mechanism [10]. Any changes in the optimal concentration of RF2 protein can have an adverse impact on the organism. For example, low RF2 concentration can decrease the termination rate in the transcript with UAA and UGA stop codons [28,29], resulting in the sequestering of ribosomes on *E. coli* transcripts. Similarly, its overproduction can lead to a premature termination of protein synthesis [10,47,48]. In this paper, we developed a simulation model of protein synthesis and mRNA degradation that explains how RF2 proteins efficiently autoregulate their concentration through programmed frameshifting. Using the model, we identified a two-layer mechanism that autoregulates RF2 protein concentration in *E. coli*. First, the RF2 synthesis rate from each mRNA transcript increases as the steady-state RF2 concentration decreases (Fig. 2). Second, a slow termination rate caused by a low RF2 concentration creates a high ribosome density on the RF2 transcript. This high ribosome density protects the transcript from nuclease digestion, thus increasing the transcript lifetime and the overall rate of RF2 synthesis (Fig. 6). The second mechanism not only contributes to the sharp autoregulatory response when RF2 concentration decreases, but also helps in minimizing the wastage of cellular resources in *E. coli*

because in the absence of the second mechanism, a lower frameshifting rate would be needed to attain an efficient sharp transition from a low to a high RF2 protein synthesis rate (Fig. 2). This would increase the unnecessary production of SPs, thus resulting in an enormous wastage of cellular resources.

In our model, we solved Eqs. (4)–(6) by assuming no time-dependent changes in J and k_d^m. However, J remains zero before the translation system achieves a steady state. Similarly, k_d^m may also evolve with time until the average ribosome density reaches a steady-state value. However, the typical timescale for an RF2 transcript to achieve a steady state is 30 s, which is significantly smaller than the mRNA lifetime (vary from 4 to 50 min; see Fig. 3) and the average time required to achieve a steady-state RF2 concentration (approximately 50 min; see Fig. S2 in [33]). This suggests that the steady-state assumption we used in solving Eqs. (4)–(6) is very unlikely to affect the overall behavior of the RF2 synthesis rate in Fig. 6.

The two essential features that are required for a sharp transition between a short and a long mRNA lifetime are the programmed frameshifting and the RF2 dependence on the translation-termination rate [Fig. 3 and Eq. (1)]. Interestingly, we also found that it is only the presence of programmed frameshifting that matters and the frameshifting rate does not contribute much to the switching between a short and a long mRNA lifetime (Fig. 3). We also found that, except for the initiation rate, other parameters that are susceptible to changes at different physiological conditions are not likely to disrupt this switching (Fig. 4). Together, these results show that the translational autoregulation by programmed frameshifting in *E. coli* is likely to remain robust against any changes in the growth conditions of *E. coli,* as long as the translation initiation remains low enough to create the LD to HD transition of ribosome traffic.

A great deal of experimental evidence shows that protein synthesis occurs in the LD regime that minimizes ribosome interference on an mRNA transcript [24,49–54], suggesting an evolutionary benefit of low initiation rate. In our study, we found that the sharp switching from a short to a long mRNA lifetime also requires RF2 transcripts to have a low initiation rate [Fig. 4(a)]. Otherwise, the transition to the HD regime at low RF2 concentration becomes a continuous transition that requires a large change in the RF2 concentration for a relatively small change in the lifetime of the RF2 transcript [Fig. 4(a)]. Therefore, the average lifetime of the RF2 transcript cannot be controlled as efficiently as in the transcript with a low initiation rate. This observation suggests an additional evolutionary benefit of a low initiation rate in the RF2 transcript that helps in achieving an efficient autoregulation of RF2 protein levels.

Translation termination kinetics determines the boundary between the allowed and forbidden regions of the steady-state RF2 concentration in *E. coli* (Fig. S5 in [33]). It has also been shown that translation termination kinetics in *E. coli* can be controlled by the post-translational modifications in the RF2 protein [55]. This suggests that, in principle, *E. coli* can tune the lower threshold of allowed steady-state RF2 concentrations through the post-translational modification enzymes.

Programmed frameshifting in release factor transcripts has been found in at least 60 different organisms, including eukaryotes [10,47,56,57]. This suggests a conserved mechanism for the autoregulation of release factor proteins across different organisms. However, the role of mRNA lifetime in the autoregulation of those release factor proteins requires further investigation. Additionally, our results show how the ribosome traffic tuned by the frameshifting mechanism can efficiently switch the mRNA from a shorter to a longer lifetime and vice versa. These results are consistent with other recent studies [58–60] which show that the ribosome density on a transcript is not merely a consequence of several regulating factors, but in some cases, it is also a tool that can regulate the gene expression.

[1] A. D. McLachlan, Annu. Rev. Phys. Chem. **23**, 165 (1972).
[2] H. Fu, R. R. Subramanian, and S. C. Masters, Annu. Rev. Pharmacol. Toxicol. **40**, 617 (2000).
[3] A. K. Sharma and E. P. O'Brien, Curr. Opin. Struct. Biol. **49**, 94 (2018).
[4] S. W. Ryter and A. M. K. Choi, Redox. Biol. **4**, 215 (2015).
[5] T. I. Lee and R. A. Young, Cell **152**, 1237 (2013).
[6] Y. Wang, P. Chakravarty, M. Ranes, G. Kelly, P. J. Brooks, E. Neilan, A. Stewart, G. Schiavo, and J. Q. Svejstrup, Proc. Natl. Acad. Sci. USA **111**, 14454 (2014).
[7] D. Bratsun, D. Volfson, L. S. Tsimring, and J. Hasty, Proc. Natl. Acad. Sci. USA **102**, 14593 (2005).
[8] V. Tyng and M. E. Kellman, J. Phys. Chem. B **123**, 369 (2019).
[9] A. De Siervi, P. De Luca, J. S. Byun, L. J. Di, T. Fufa, C. M. Haggerty, E. Vazquez, C. Moiola, D. L. Longo, and K. Gardner, Cancer Res. **70**, 532 (2010).
[10] R. Betney, E. de Silva, J. Krishnan, and I. Stansfield, RNA **16**, 655 (2010).
[11] A. D. Petropoulos, M. E. McDonald, R. Green, and H. S. Zaher, J. Biol. Chem. **289**, 17589 (2014).
[12] W. J. Craigen and C. T. Caskey, Nature (London) **322**, 273 (1986).
[13] C. Deneke, R. Lipowsky, and A. Valleriani, Phys. Biol. **10**, 046008 (2013).
[14] F. Braun, J. Le Derout, and P. Régnier, EMBO J. **17**, 4790 (1998).
[15] A. Deana and J. G. Belasco, Genes Dev. **19**, 2526 (2005).
[16] M. Pedersen, S. Nissen, N. Mitarai, S. Lo Svenningsen, K. Sneppen, and S. Pedersen, J. Mol. Biol. **407**, 35 (2011).
[17] A. K. Sharma and D. Chowdhury, Biophys. Rev. Lett. **07**, 135 (2012).
[18] R. K. P. Zia, J. J. Dong, and B. Schmittmann, J. Stat. Phys. **144**, 405 (2011).
[19] J. J. Dong, B. Schmittmann, and R. K. P. Zia, Phys. Rev. E **76**, 051113 (2007).
[20] A. K. Sharma and D. Chowdhury, J. Theor. Biol. **289**, 36 (2011).
[21] A. K. Sharma and E. P. O'Brien, J. Phys. Chem. B **121**, 6775 (2017).
[22] R. J. Harris and R. B. Stinchcombe, Phys. Rev. E **70**, 016108 (2004).

[23] V. Yadav, R. Singh, and S. Mukherji, J. Stat. Mech. (2012) P04004.
[24] A. K. Sharma, P. Sormanni, N. Ahmed, P. Ciryam, U. A. Friedrich, G. Kramer, and E. P. O'Brien, PLoS Comput. Biol. **15**, e1007070 (2019).
[25] A. K. Sharma, N. Ahmed, and E. P. O'Brien, Phys. Rev. E **97**, 022409 (2018).
[26] D. E. Weinberg, P. Shah, S. W. Eichhorn, J. A. Hussmann, J. B. Plotkin, and D. P. Bartel, Cell Rep. **14**, 1787 (2016).
[27] M. P. Hui, P. L. Foley, and J. G. Belasco, Annu. Rev. Genet. **48**, 537 (2014).
[28] M. Y. Pavlov, D. V Freistroffer, V. Dincbas, J. MacDougall, R. H. Buckingham, and M. Ehrenberg, J. Mol. Biol. **284**, 579 (1998).
[29] V. Dinçbas-Renqvist, Å. Engström, L. Mora, V. Heurgué-Hamard, R. Buckingham, and M. Ehrenberg, EMBO J. **19**, 6900 (2000).
[30] J. M. Berg, J. L. Tymoczko, and L. Stryer, *Biochemistry* (Freeman, New York, 2002), p. 1120.
[31] P. Ciryam, R. I. Morimoto, M. Vendruscolo, C. M. Dobson, and E. P. O'Brien, Proc. Natl. Acad. Sci. USA **110**, E132 (2013).
[32] D. T. Gillesple, J. Phys. Chem. **81**, 2340 (1977).
[33] See Supplemental Material at http://link.aps.org/supplemental/10.1103/PhysRevE.103.062412 for details.
[34] N. T. Ingolia, S. Ghaemmaghami, J. R. S. Newman, and J. S. Weissman, Science **324**, 218 (2009).
[35] M. A. Moran, B. Satinsky, S. M. Gifford, H. Luo, A. Rivers, L.-K. Chan, J. Meng, B. P. Durham, C. Shen, V. A. Varaljay, C. B. Smith, P. L. Yager, and B. M. Hopkinson, ISME J. **7**, 237 (2013).
[36] J. B. Andersen, C. Sternberg, L. K. Poulsen, S. P. Bjørn, M. Givskov, and S. Molin, Appl. Environ. Microbiol. **64**, 2240 (1998).
[37] L. B. Shaw, R. K. P. Zia, and K. H. Lee, Phys. Rev. E **68**, 021910 (2003).
[38] A. K. Sharma and D. Chowdhury, Phys. Rev. E **82**, 031912 (2010).
[39] A. K. Sharma and D. Chowdhury, Phys. Biol. **8**, 026005 (2011).
[40] A. Garai, D. Chowdhury, D. Chowdhury, and T. V Ramakrishnan, Phys. Rev. E **80**, 011908 (2009).
[41] J. Estrada, F. Wong, A. DePace, and J. Gunawardena, Cell **166**, 234 (2016).
[42] J. J. Hopfield, Proc. Natl. Acad. Sci. U.S.A. **71**, 4135 (1974).
[43] P. Goloubinoff, A. S. Sassi, B. Fauvet, A. Barducci, and P. De Los Rios, Nat. Chem. Biol. **14**, 388 (2018).
[44] G. Csárdi, A. Franks, D. S. Choi, E. M. Airoldi, and D. A. Drummond, PLoS Genet. **11**, e1005206 (2015).
[45] H. Chen, K. Shiroguchi, H. Ge, and X. S. Xie, Mol. Syst. Biol. **11**, 808 (2015).
[46] E. C. A. Goodall, A. Robinson, I. G. Johnston, S. Jabbari, K. A. Turner, A. F. Cunningham, P. A. Lund, J. A. Cole, and I. R. Henderson, MBio. **9**, e02096 (2018).
[47] T. Nyikó, A. Auber, L. Szabadkai, A. Benkovics, M. Auth, Z. Mérai, Z. Kerényi, A. Dinnyés, F. Nagy, and D. Silhavy, Nucleic Acids Res. **45**, 4174 (2017).
[48] Y. Kobayashi, J. Zhuang, S. Peltz, and J. Dougherty, J. Biol. Chem. **285**, 19776 (2010).
[49] Y. Arava, Y. Wang, J. D. Storey, C. L. Liu, P. O. Brown, and D. Herschlag, Proc. Natl. Acad. Sci. USA **100**, 3889 (2003).
[50] L. Ciandrini, I. Stansfield, and M. C. Romano, PLoS Comput. Biol. **9**, e1002866 (2013).
[51] M. Siwiak and P. Zielenkiewicz, PLoS One **8**, e73943 (2013).
[52] G. Shaham and T. Tuller, DNA Res. **25**, 195 (2018).
[53] A. Pai and L. You, Mol. Syst. Biol. **5**, 286 (2009).
[54] D. Kennell and H. Riezman, J. Mol. Biol. **114**, 1 (1977).
[55] L. Mora, V. Heurgué-Hamard, M. de Zamaroczy, S. Kervestin, and R. H. Buckingham, J. Biol. Chem. **282**, 35638 (2007).
[56] R. Betney, E. De Silva, C. Mertens, Y. Knox, J. Krishnan, and I. Stansfield, RNA **18**, 2320 (2012).
[57] P. V. Baranov, R. F. Gesteland, and J. F. Atkins, EMBO Rep. **3**, 373 (2002).
[58] V. Presnyak, N. Alhusaini, Y. Chen, S. Martin, N. Morris, N. Kline, S. Olson, D. Weinberg, K. E. Baker, B. R. Graveley, and J. Coller, Cell **160**, 1111 (2015).
[59] M. W. Webster, Y. H. Chen, J. A. W. Stowell, N. Alhusaini, T. Sweet, B. R. Graveley, J. Coller, and L. A. Passmore, Mol. Cell **70**, 1089 (2018).
[60] J. D. Richter and J. Coller, Cell **163**, 292 (2015).